DOI: 10.1007/s11099-015-0153-y PHOTOSYNTHETICA 54 (1): 40-46, 2016

Comparison of the photosynthetic characteristics in the pericarp and flag leaves during wheat (*Triticum aestivum* L.) caryopsis development

L.A. KONG[*,+], Y. XIE[*], M.Z. SUN[**], J.S. SI[*] and L. HU[*]

Crop Research Institute, Shandong Academy of Agricultural Sciences, 202 Gongyebei Road, Jinan 250100, China[*]
Plant Protection Station of Liaocheng City, Liaocheng 252000, China[**]

Abstract

The pericarp of cereal crops is considered a photosynthetically active tissue. Although extensive studies have been performed on green leaves, the photosynthetic role of the pericarp in cereal caryopsis development has not been well investigated. In the present study, we investigated the anatomy, ultrastructure, chlorophyll (Chl) fluorescence, and oxygen evolution of the pericarp during caryopsis ontogenesis in field wheat (*Triticum aestivum* L.). The results showed that wheat pericarp cross-cells contained Chl; the grana stacks and thylakoid membranes in the cross-cells were more distinct in the pericarp than those in the flag leaves as shown by transmission electron microscopy. Chl fluorescence revealed that the photosynthetic efficiency, which was indicated by values of maximum efficiency of PSII photochemistry and effective PSII quantum yield, was lower in the pericarp compared to that of the flag leaf eight days after anthesis (DAA), whereas similar values were subsequently observed. The nonphotochemical quenching values were lower from 8–16 DAA but significantly increased in the pericarp from 24–32 DAA compared to the flag leaf. The oxygen evolution rate of the flag leaves was consistently higher than that of pericarp; notably, isolated pericarps released more oxygen than intact pericarps during caryopsis development. These results suggest that the pericarp plays a key role in caryopsis development by performing photosynthesis as well as by supplying oxygen to the endosperm and dissipating excessive energy during the grain-filling stages.

Additional key words: chlorophyll fluorescence; oxygen evolution; pericarp; photosynthesis; wheat; ultrastructure.

Introduction

Green leaves predominantly utilize atmospheric CO_2 and are commonly considered the primary source of photosynthetic assimilates, whereas Chl-containing fertile flower organs, fruits, and other tissues are principally considered to perform nonphotosynthetic functions. However, an increasing body of evidence has demonstrated that higher plants have the potential to use non-leaf green organs to perform photosynthetic CO_2 assimilation (Aschan and Pfanz 2003, Kong *et al.* 2010). The photosynthesis of certain non-leaf organs, such as ears, includes two processes: assimilation of atmospheric CO_2 and photosynthetic refixation of respiratory CO_2.

The refixation of respired CO_2 could markedly impact the crop grain yield by minimizing the loss of CO_2 because CO_2 recycling is relatively independent of ambient conditions. Compared to the flag leaves, ear organs have higher relative water content with better osmotic adjustment under water stress, and this capacity might prolong the duration of photosynthetic activity in the ears during grain-filling (Tambussi *et al.* 2007). In barley (*Hordeum vulgare* L.) and wheat (*Triticum aestivum* L.), ear photosynthesis contributes 10 and 76% of the assimilation, respectively, to grain-filling (Araus *et al.* 1993, Aschan and Pfanz 2003). In wheat,

Received 16 December 2014, *accepted* 20 April 2015, *published as online first* 18 June 2015.
[+]Corresponding author; phone: 0086-531-83178123, fax: 0086-531-88619088, e-mail: kongling-an@163.com
Abbreviations: Chl – chlorophyll; DAA – days after anthesis; F_0 – minimal fluorescence yield of the dark-adapted state; F_s – steady-state fluorescence yield; F_v – maximum variable fluorescence in dark-adapted samples; F_v/F_m – maximal quantum yield of PSII photochemistry; F_m – maximal fluorescence yield of the dark-adapted state; FM – fresh mass; F_m' – maximal fluorescence yield of the light-adapted state; NPQ – nonphotochemical quenching; PEPC – phospho*enol*pyruvate carboxylase; Φ_{PSII} – effective quantum yield of PSII photochemistry.
Acknowledgments: This study was funded through grants from the Shandong Modern Agricultural Technology & Industry System (SDAIT-04-022-02), Modern Agro-Industry Technology Research System (CARS-3-1-21), Specialized Agroscientific Research Fund for Public Causes, Ministry of Agriculture of the People's Republic of China (201303109-7, 201203079 and 201203053-2) and the Program of Major Independently Innovative Key Technology of Shandong Province (2014GJJS0201).

photosynthesis in Chl-containing layers of pericarp accounted for approximately 40–42% of the total ear photosynthesis (Evans and Rawson 1970, Watson and Duffus 1988). The pericarp of cereal caryopses retrieved internally produced CO_2 according to light conditions, and this process was more important than atmospheric CO_2 fixation (Watson and Duffus 1988, Caley *et al.* 1990, Watson and Duffus 1991). Interestingly, Nutbeam and Duffus (1976, 1978) reported that the pericarp had considerably lower Rubisco carboxylase activity than that of phospho*enol*pyruvate carboxylase (PEPC); in addition, fed $^{14}CO_2$ can be rapidly incorporated into C_4-acid (malic acid), suggesting that the C_4 pathway might be a main pathway in the pericarp.

Hypoxia is a phenomenon that occurs in seeds of both monocotyledonous and dicotyledonous species (van Dongen *et al*. 2004), where the developing caryopsis becomes increasingly energy-limited during early stages; it largely reflects elevated metabolic activity that leads to increased energy demand (Sreenivasulu *et al.* 2010). However, low internal oxygen affects assimilate transport *via* the phloem and reduces caryopsis metabolism in barley and wheat (van Dongen *et al.* 2004, Sreenivasulu *et al.* 2010). Therefore, it remains unknown whether pericarp photosynthesis supplies oxygen to the endosperm. In addition, heat stress frequently occurs at the later stages of wheat grain-filling in northern China. However, it is unclear whether the pericarp is involved in the photoprotective mechanisms by dissipating excessive energy in order to resist heat stress.

The objective of the present study was to compare photosynthetic characteristics of the pericarp with those of the flag leaves. In addition, the role of pericarp photosynthesis in supplying oxygen during the filling stages and dissipating excessive energy were examined to elucidate potential functions of pericarp photosynthesis in caryopsis ontogeny. Our results might help elucidate the functions of the pericarp during caryopsis development.

Materials and methods

Plant material: The experiment was performed during the winter wheat growing seasons of 2013–2014 at an experimental station (36°42'N, 117°4'E; 48 m a.s.l.) at the Shandong Academy of Agricultural Sciences, China. The winter wheat cultivar Jimai 22 was used for the experiments.

Observation of caryopsis structure: Immature caryopses were harvested 20 DAA during the middle stage of grain-filling for light microscopy specimen preparation. The caryopses were manually cut using a blade, and the slices were placed on a glass slide. Subsequently, the sections were visualized using a fluorescence microscope (*DM2500*, *Leica Microsystems*, Wetzlar, Germany), and images were acquired with a *Leica DFC420* digital camera (*Leica Microsystems*). Chl autofluorescence was excited at 488 nm and emissions were collected from 685 to 740 nm.

Scanning electron microscopy: Caryopsis-containing dorsal pericarps were cut into 3 mm × 2 mm sections and immediately fixed in 2.5% (v/v) glutaraldehyde solution in 100 mM sodium phosphate buffer (SPB) (pH 7.2) for 24 h. The sections were then dehydrated in ethanol series, and critical drying occurred under CO_2 atmosphere. The samples were sputter coated with gold (~20 nm) and observed using a scanning electron microscope (SEM; *XL30*, *Philips*, Eindhoven, the Netherlands).

Transmission electron microscopy: The pericarp and flag leaf samples were collected at 8, 16, 24, and 32 DAA, cut into 1 mm^3 sections and immediately fixed in 2.5% (v/v) glutaraldehyde solution in 100 mM SPB (pH 7.2) for 24 h. After washing with 100 mM SPB, the samples were post-fixed with 1% (w/v) osmium tetroxide in SPB at 4°C for 4 h. The samples were subsequently dehydrated in a graded ascending ethanol serie, transferred into propylene oxide, and embedded in *Epon 812* resin (*Shell Chemical*, Houston, TX, USA). Semi-thin transverse sections (2 μm thick) were cut using an *LKB-V* microtome (*LKB*, Bromma, Sweden) and stained with toluidine blue O. The structure of the cross-cells was observed and photographed using a light microscope (*Zeiss Axioskop 40*, *Leica*, Germany) equipped with a digital camera. Ultrathin sections (70 nm) were cut using an *LKB-V* microtome and mounted on a Formvar-coated brass grid. The sections were stained with 2% uranyl acetate (w/v) in 70% methanol (v/v) and 0.5% lead citrate. The preparations were observed using a *JEM-1230* transmission electron microscope (*JEOL Ltd*., Tokyo, Japan) at 80 kV.

Chl fluorescence analysis: The Chl fluorescence measurements were performed at 8, 16, 24, and 32 DAA to determine the maximum PSII quantum yield (F_v/F_m), effective PSII quantum yield (Φ_{PSII}), and nonphotochemical quenching (NPQ) parameters in caryopses and flag leaves. The Chl fluorescence induction kinetics was measured at room temperature using a kinetic imaging fluorometer (*FluorCam*, *Photon Systems Instruments Ltd*., Brno, Czech Republic) according to Nedbal *et al*. (2000). After measuring the minimum fluorescence in the dark-adapted state (F_0), the samples were illuminated with a saturating pulse (1,500 μE m^2 s^{-1}) to determine the maximal fluorescence in the dark-adapted state (F_m). The samples were subsequently illuminated with actinic light using saturating flashes of 0.7 s. The maximum fluorescence (F_m') and steady-state fluorescence (F_s) of light-

adapted leaves were recorded. Numerical analyses of the classical physiological parameters were performed on the maximum PSII quantum yield, $F_v/F_m = (F_m - F_0)/F_m$, quantum efficiency of PSII electron transport, $\Phi_{PSII} = (F_m' - F_s)/F_m'$, and nonphotochemical Chl fluorescence quenching parameter, $NPQ = (F_m - F_m')/F_m'$. The fluorescence parameters were calculated using the *FluorCam* software (*version 6*) according to the manufacturer's instructions. The Chl fluorescence emission transients were captured using a charge-coupled device (CCD) camera in a series of images with a resolution of 512 × 512 pixels.

Oxygen evolution rate: The flag leaf and pericarp samples (~40 mg) were placed into the reaction cup of an oxygen electrode. To isolate the pericarp, the kernel was longitudinally cut and endosperm and embryo were removed using a razor blade. The rates of oxygen evolution from the samples were measured in the reaction mixture (50 mM Tris-HCl and 20 mM $NaHCO_3$, pH 7.2) at room temperature using an *Oxy-lab* O_2 electrode (*Hansatech*, Cambridge, UK). The oxygen exchange in both flag leaves and pericarps was assayed under dark and light conditions during caryopsis development. For intact pericarps, the caryopsis value was transformed to the pericarp value by multiplying the fresh mass (FM) ratio of pericarp to caryopsis. The rate of oxygen evolution was expressed in μmol mg^{-1}(FM) min^{-1}, and the data were averaged from eight replications.

Statistical analysis: A statistical analysis was performed using *Data Processing System* (DPS) statistical software (*v.14.10*, *Refine Information Tech. Co., Ltd*., Hangzhou, Zhejiang, China) (Tang and Zhang 2013), and a one-way analysis of variance (*ANOVA*) was used to detect differences between means using *Tukey*'s test at $P<0.05$. The data were presented as the mean ± standard deviation, and significant differences among treatments were indicated with different letters. In addition, a statistical analysis was also conducted to assess the differences among DAA.

Results

Distribution of Chl in caryopsis: The emission of autofluorescence under a fluorescence microscope localized Chl in plant tissue. A transverse section of caryopsis showed that the pericarp cross-cells contained Chl, which was present in a distinct layer within the pericarp (so-called chlorenchyma) and covered the entire endosperm (Fig. 1*A*,*B*). The epidermis consisted of elongated cells with sinuous walls. However, stomata were not observed on the pericarp surface (Fig. 1*C*).

Ultrastructure of the pericarp at different stages: At 8 DAA, the pericarp chloroplasts of wheat plants were spindle-like with well stacked thylakoids and accumulated starch grains (Fig. 2*A*,*B*). In addition, the cross-cell chloroplast possessed well defined grana and stroma lamellae, and the cross-cell wall was markedly thin. Although the chloroplasts in the pericarp were smaller, the thylakoids were well stacked compared to the flag leaf (Fig. 2*C*). At 16 DAA, ultrastructural variability of the chloroplasts in the pericarp was observed, and the cross-cells were highly vacuolated, with many mitochondria pressed to the cell wall. The cross-cell wall, particularly the outer wall, was significantly thickened, and a pit field was observed. At this stage, numerous

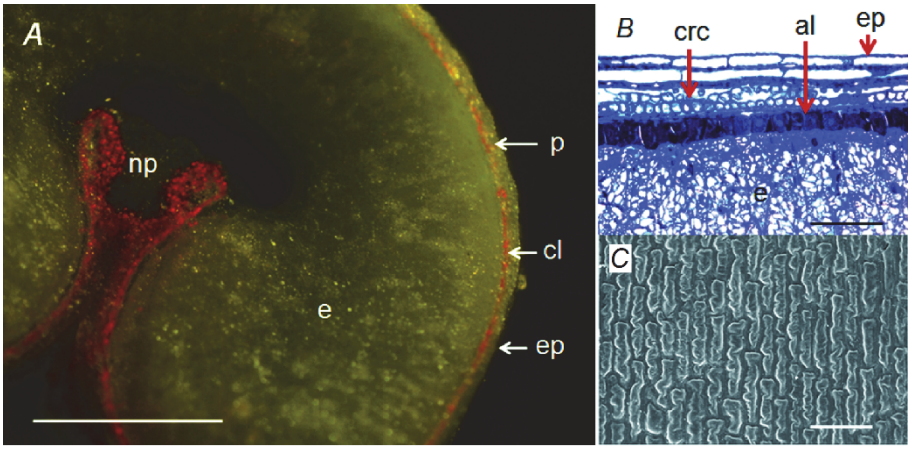

Fig. 1. Microscopic images of caryopses of cv. Jimai 22 at 20 DAA. (*A*) Free-hand transverse section of the caryopsis showing red Chl autofluorescence in cross-cells after blue excitation; (*B*) abdominal region containing the pericarp; and (*C*) scanning electron micrograph showing the morphology of the caryopsis epidermis. Stomata were not observed on the epidermis. al – aleurone layer, cl – Chl layer; crc – cross-cells; e – endosperm; ep – epidermis; p – pericarp; np – nucellar projection. Scale bars: (*A*) 1 cm, (*B*) 1 mm, and (*C*) 100 μm.

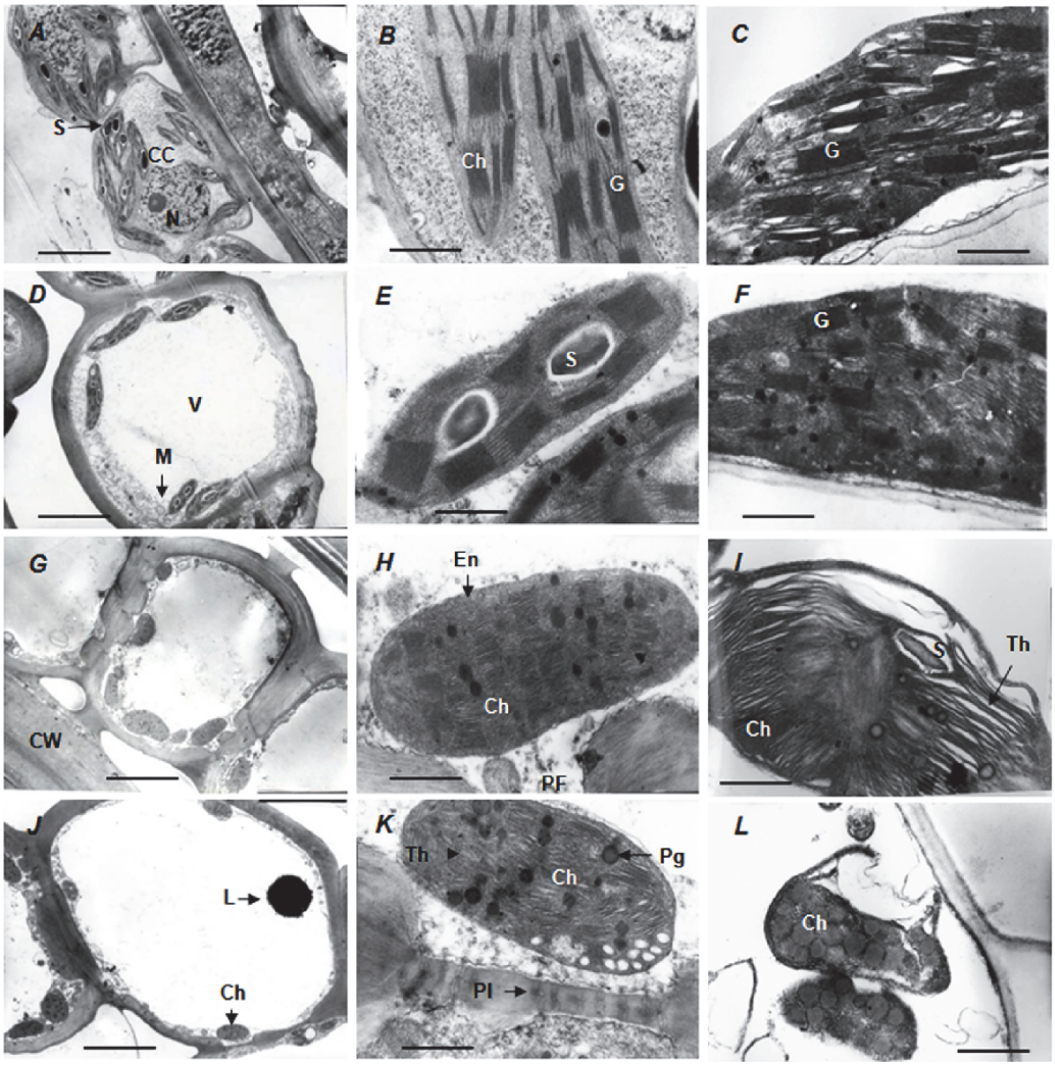

Fig. 2. Transmission electron microscopy images showing the ultrastructure of cross-cells in the caryopsis pericarp (*A*, *B*, *D*, *E*, *G*, *H*, *J*, *K*) and cells in the flag leaf (*C*, *F*, *I*, *L*) at 8, 16, 24, and 32 DAA in wheat. (*A*, *B*, *C*): 8 DAA; (*D*, *E*, *F*): 16 DAA; (*G*, *H*, *I*): 24 DAA, (*J*, *K*, *L*): 32 DAA. (*B*), (*E*), (*H*), and (*K*): higher magnification of the partial areas shown in (*A*), (*D*), (*G*), and (*J*), respectively. Ch – chloroplast; CW – cell wall; En – envelop; G – granum; L – lipid; Pg – plastoglobuli; PF – pit field; Pl – plasmodesma; S – starch; Th – thylakoid; V – vacuole. Scale bars: (*A*, *D*, *G*, and *J*) 5 μm and (*B*, *C*, *E*, *F*, *H*, *I*, *K*, and *L*) 500 nm.

starch grains were observed within the chloroplasts (Fig. 2*D*,*E*). At 24 DAA, the pericarp chloroplasts were elliptical in shape and had indistinctively stacked thylakoids and fewer starch grains. The partial thylakoid membrane system of the chloroplasts was disorganized, and the thylakoids of the grana were indistinctly discriminated (Fig. 2*G*,*H*). However, the grana in these cells were abundant compared to those of the flag leaf (Fig. 2*I*). At 32 DAA, the cross-cell contained few elliptical chloroplasts with no starch grains. However, the membrane system of these chloroplasts was more intact than expected. The most striking feature at this stage was the frequently observed plasmodesmata between adjoining cross-cells as well as between cross-cells and inner cells. The number of plastoglobuli in the chloroplast increased and the nucleus disappeared in almost all cells. Although the grana were not irregularly stacked and certain thylakoids were indistinguishable, more intact chloroplasts were observed (Fig. 2*J*,*K*) compared to those of the flag leaves (Fig. 2*L*).

Chl fluorescence: The caryopsis is green because the cross-cells of the pericarp contain Chl. For Chl fluorescence measurements, the flag leaves were used as controls. The ratio of F_v/F_m in the flag leaf and caryopsis slowly declined from 8 to 16 DAA, which was followed by a significant decline at 24 DAA and a sharp decline at 32 DAA (Fig. 3*A*,*D*). The maximum values of Φ_{PSII} for both the flag leaf and caryopsis were observed at 16 DAA which was followed by a slight decline at 24 DAA and by the dramatic decline at 32 DAA (Fig. 3*B*,*E*). Significant differences in the values for both parameters were

observed at 8 DAA between the flag leaf and caryopsis. In contrast, the NPQ coefficient increased during caryopsis development, and the NPQ values in the caryopsis were significantly lower at 8 and 16 DAA and significantly higher at 24 and 32 DAA compared to that of the flag leaves. Specifically, the NPQ value for the caryopsis was more than 2-fold higher than the value for the flag leaf at 32 DAA (ripening stage) under the high-temperature conditions in northern China.

Interestingly, the heterogeneous variability in the NPQ across the leaf area was consistent with the F_v/F_m value, and in regions with a relatively high F_v/F_m, the NPQ increased, whereas in regions with a low F_v/F_m, the NPQ values were low (Fig. 3*A*,*C*).

Rate of oxygen evolution in wheat caryopsis: The photosynthetic capacity evaluation of the wheat caryopsis pericarp was based on different rates of oxygen exchange under light or dark conditions. During the grain-filling stages, the oxygen evolution rate in the flag leaves was consistently higher than those in both intact and isolated caryopsis pericarps (Fig. 4). However, variations in the rate of photosynthetic oxygen evolution differed between the pericarp and flag leaf at the different developmental

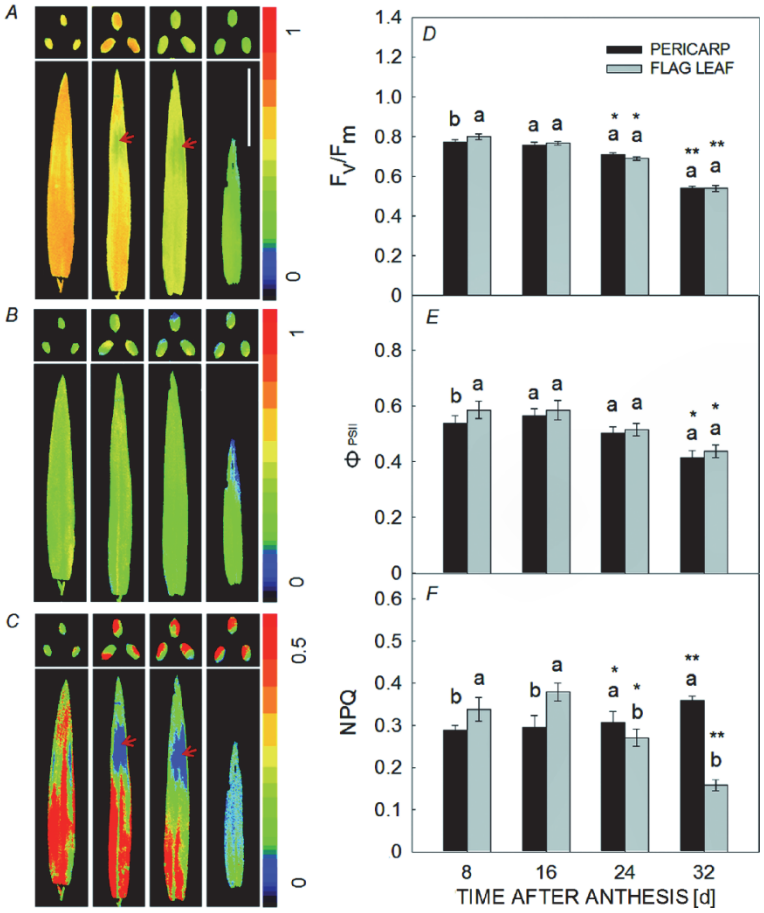

Fig. 3. Changes in the Chl fluorescence parameters in flag leaves and caryopses during the grain-filling period in wheat: (*A*,*D*) F_v/F_m, (*B*,*E*) Φ_{PSII}, and (*C*,*F*) NPQ. *A*,*B*,*C*: Representative pseudocolored images showing the F_v/F_m, Φ_{PSII}, and NPQ, respectively, of the caryopses and flag leaves. Bar = 5 cm. *D*,*E*,*F*: Temporal changes in the F_v/F_m, Φ_{PSII}, and NPQ values, respectively, for caryopses and flag leaves at different stages. Each data point in the figure represents the average and standard deviation of at least ten individually selected and analyzed samples. The parameters calculated for the caryopsis and flag leaf significantly differed at the $P<0.05$, which is indicated with *different letters*. *, ** – significance at the 0.05 and 0.01 probability levels, respectively, at 16, 24, or 32 DAA compared with those at 8 DAA. F_v/F_m – maximum PSII quantum yield; Φ_{PSII} – effective PSII quantum yield.

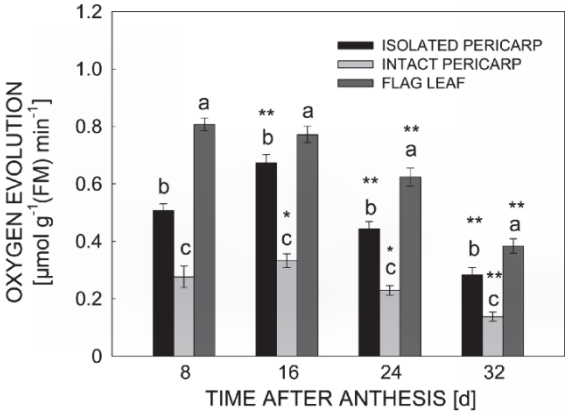

Fig. 4. Temporal changes in the rate of oxygen evolution in pericarps and flag leaves at different stages. Each value represents the average of six measurements. *, ** – the significance at the 0.05 and 0.01 probability levels, respectively, at 16, 24, or 32 DAA compared with those at 8 DAA.

stages. The oxygen evolution rate continually decreased in the flag leaf; the peak oxygen evolution rate [0.637 μmol g^{-1}(FM) min^{-1}] was observed at 16 DAA and then it was continually declining during the later stages in the pericarp. At the ripening stage, the oxygen evolution rate in the flag leaves were 1.36- and 2.80-fold higher than that of the isolated and intact pericarps, respectively.

Throughout the grain-filling stages, the rate of oxygen evolution was significantly lower in the intact pericarps than that in the isolated pericarps, indicating that a large amount of oxygen was transferred to the inner parts of the developing caryopsis. These results suggest that at least partial oxygen production occured within the caryopsis through pericarp photosynthesis.

Discussion

The Chl-containing cells of caryopses showed high rates of photosynthesis (Wang *et al.* 1989), and these cells show C_4 photosynthesis (Duffus and Rosie 1973, Nutbeam and Duffus 1976, Watson and Duffus 1991). Our results showed that the pericarp green layer of wheat was located between the endosperm and the outer transparent layer (Fig. 1*A*,*B*). Stomata were not observed in either the transverse sections (Fig. 1*A*) or scanning electron micrographs of the caryopsis epidermis (Fig. 1*C*), suggesting that the outer pericarp tissue might be relatively impermeable to CO_2 and O_2. Therefore, a characterization of pericarp photosynthesis during caryopsis ontogeny in wheat was required.

As the outer pericarp of immature caryopses exhibited high PEPC activity in durum wheat (Araus *et al.* 1993) and the external layer of the pericarp has lower impermeability, it is reasonable to suggest that external CO_2 might not be sufficient and caryopsis-evolved CO_2 may be used for photosynthesis. Indeed, Watson and Duffus (1988) observed that only ~2% of the starch mass was attributed to the fixation of external CO_2 in mature caryopses, suggesting that the photosynthetic fixation of CO_2 in the pericarp is likely caused by the recapture of endosperm respiration-derived CO_2 and refixation of a significant portion of its own respiratory CO_2 by the caryopsis (Evans and Rawson 1970). In the present study, we observed that during the early stages of development, the chloroplasts in the cross-cells contained a high number of well stacked grana. During the later stages of development, the chloroplasts in the cross-cells remained intact in structure, whereas the chloroplasts in the flag leaf cells were nearly disrupted. It revealed that caryopses are photosynthetically active organs in wheat and provide photosynthetic assimilates to the endosperm during the grain-filling.

Chl fluorescence measurement is an important noninvasive technique for the assessment and quantification of PSII activity in photosynthetic organs. Because PSII is primarily localized in the stacked thylakoid membranes in chloroplasts, these membranes are closely associated with the photosynthetic rate. Thus, F_v/F_m, and Φ_{PSII} provide useful indices for the evaluation of photochemistry in green tissues. In the present study, the values for F_v/F_m and Φ_{PSII} confirmed that both parameters were significantly lower in caryopses than those in the flag leaves at 8 DAA; however, at subsequent stages, no differences were observed between these organs, indicating that the pericarp efficiently utilized light through PSII.

NPQ is associated with the de-excitation of the singlet-excited state in light-harvesting antenna of PSII and it is a mechanism that protects photosynthetic organisms against excessive light energy (Demmig-Adams 1990, Kotabová *et al.* 2011, Demmig-Adams *et al.* 2012). Interestingly, we observed that the NPQ values remained high at 24 to 32 DAA, a phase with higher than optimum temperatures for wheat growth in northern China. Although the caryopsis is not fully exposed to sunlight, this organ receives 1/8 to 1/4 of the light intensity (Wang *et al.* 1989). Considering that the caryopsis is a well developed organ containing tender tissues, it is tempting to suggest that NPQ in the caryopsis serves as an effective photoprotective mechanism in wheat.

Because of the low permeability of the seed coat and high sink metabolism for storage product accumulation, caryopsis development might be limited by the low internal O_2 concentration, which indicates the low import rate of assimilates *via* phloem (van Dongen *et al.* 2004). Thus, it is reasonable to speculate that oxygen delivery to the endosperm *via* pericarp photosynthesis is crucial for respiratory ATP synthesis (Cochrane and Duffus 1979, Rolletschek *et al.* 2003, 2004; Sreenivasulu *et al.* 2010). Indeed, the synthesis of storage products with high-energy demand preferentially occurs in regions with favorable oxygen supplies (Neuberger *et al.* 2008). Xiong *et al*. (2013) inferred that rapid photosynthesis occurs in the abdominal pericarp to meet the needs of vascular tissue for energy and oxygen. The rate of oxygen evolution was used as an indicator of the photosynthetic capacity and respiratory activity of the caryopsis (Caley *et al*. 1990). In the present study, although light-dependent oxygen evolution in the caryopses or isolated pericarps was lower than that of the flag leaves (Fig. 4), these structures had strong structural bases for photosynthesis (Fig. 2) and similar values of F_v/F_m and Φ_{PSII}; therefore, the pericarps possessed higher photosynthetic activity during grain-filling. Importantly, we observed that isolated pericarp evolved a large amount of oxygen relative to the intact pericarp; it suggests that a greater quantity of O_2 might be delivered to the endosperm for respiratory processes. However, compared to the results of the Chl fluorescence analysis, the rate of oxygen evolution, even in the isolated pericarps, was significantly lower than that in the flag leaves, suggesting that diffusion of the produced oxygen towards the outside of caryopsis might be limited by the impermeable external layer, which represented a physical barrier restricting O_2 release.

In summary, the caryopsis showed distinct structural

characteristics for photosynthesis and the photosynthetic activity in the pericarp provided not only carbohydrates but also oxygen to the developing caryopsis. In addition, the values of Chl fluorescence parameters suggest that the pericarp might function to dissipate excessive energy when subjected to heat stress during grain-filling. Thus, it is reasonable to suggest that caryopsis ontogeny is at least partially regulated through oxygen derived from green-layer photosynthesis and photoprotective mechanisms of the pericarp.

References

Araus J.L., Bort J. Brown R.H. *et al.*: Immunocytochemical localization and photosynthetic gas exchange characteristics in ears of *Triticum durum* Desf. – Planta **191**: 507-514, 1993.

Aschan G., Pfanz H.: Non-foliar photosynthesis – a strategy of additional carbon acquisition. – Flora **198**: 81-97, 2003.

Caley C.Y., Duffus C.M., Jeffcoat B.: Photosynthesis in the pericarp of developing wheat grains. – J. Exp. Bot. **41**: 303-307, 1990.

Cochrane M.P., Duffus C.M.: Morphology and ultrastructure of immature cereal grains in relation to transport. – Ann. Bot.-London **44**: 67-72, 1979.

Demmig-Adams B.: Carotenoids and photoprotection in plants: a role for the xanthophyll zeaxanthin. – BBA-Bioenergetics **1020**: 1-24, 1990.

Demmig-Adams B., Cohu C.M., Muller O. *et al.*: Modulation of photosynthetic energy conversion efficiency in nature: from seconds to seasons. – Photosynth. Res. **113**: 75-88, 2012.

Duffus C.M., Rosie R.: Some enzyme activities associated with the chlorophyll containing layers of the immature barley pericarp. – Planta **114**: 219-226, 1973.

Evans L.T., Rawson H.M.: Photosynthesis and respiration by the flag leaf and component of the ear during grain development in wheat. – Aust. J. Biol. Sci. **23**: 245-254, 1970.

Kong L., Wang F., Feng B.: The structural and photosynthetic characteristics of the exposed peduncle of wheat (*Triticum aestivum* L.): an important photosynthate source for grain-filling. – BMC Plant Biol. **10**: 141, 2010.

Kotabová E., Kaňa R., Jarešová J., Prášil O.: Non-photochemical fluorescence quenching in *Chromera velia* is enabled by fast violaxanthin de-epoxidation. – FEBS Letters **585**: 1941-1945, 2011.

Nedbal L., Soukupová J., Kaftan D. *et al.*: Kinetic imaging of chlorophyll fluorescence using modulated light. – Photosynth. Res. **66**: 3-12, 2000.

Neuberger T., Sreenivasulu N., Rokitta M.: Quantitative imaging of oil storage in developing crop seeds. – Plant Biotechnol. J. **6**: 31-45, 2008.

Nutbeam, A.R., Duffus, C.M.: Evidence for C_4 photosynthesis in barley pericarp tissue. – Biochem. Bioph. Res. Co. **70**: 1198-1203, 1976.

Nutbeam A.R., Duffus C.M.: Oxygen exchange in the pericarp green layer of immature cereal grains. – Plant Physiol. **62**: 360-362, 1978.

Rolletschek H., Weber H., Borisjuk L. *et al.*: Energy status and its control on embryogenesis of legumes. Embryo photosynthesis contributes to oxygen supply and is coupled to biosynthetic fluxes. – Plant Physiol. **132**: 1196-1206, 2003.

Rolletschek H., Weschke W., Weber H. *et al.*: Energy state and its control on seed development: starch accumulation is associated with high ATP and steep oxygen gradients within barley grains. – J. Exp. Bot. **401**: 1351-1359, 2004.

Sreenivasulu N., Borisjuk L., Junker B.H. *et al.*: Barley grain development: toward an integrative view. – Int. Rev. Cel. Mol. Bio. **281**: 49-89, 2010.

Tambussi E.A., Bort J., Guiamet J.J. *et al.*: The photosynthetic role of ears in C_3 cereals: metabolism, water use efficiency and contribution to grain yield. – CRC Cr. Rev. Plant Sci. **26**: 1-16, 2007.

Tang Q.Y., Zhang C.X.: Data Processing System (DPS) software with experimental design, statistical analysis and data mining developed for use in entomological research. – Insect Sci. **20**: 254-260, 2013.

van Dongen J.T., Roeb G.W., Dautzenberg M. *et al.*: Phloem import and storage metabolism are highly coordinated by the low oxygen concentrations within developing wheat seeds. – Plant Physiol. **135**: 1809-1821, 2004.

Wang X.D., Jin S.P., Zhang W.C.: [Synthesis and distribution of assimilates in the green layer of pericarp of developing wheat caryopsis.] – Acta Phytophysiol. Sinica **15**: 69-75, 1989. [In Chinese]

Watson P.A., Duffus C.M.: Carbon dioxide fixation by detached cereal caryopses. – Plant Physiol. **87**: 504-509, 1988.

Watson P.A., Duffus C.M.: Light-dependent CO_2 retrieval in immature barley caryopses. – J. Exp. Bot. **42**: 1013-1019, 1991.

Xiong F., Yu X.R., Zhou L. *et al.*: Structural and physiological characterization during wheat pericarp development. – Plant Cell Rep. **32**: 1309-1320, 2013.